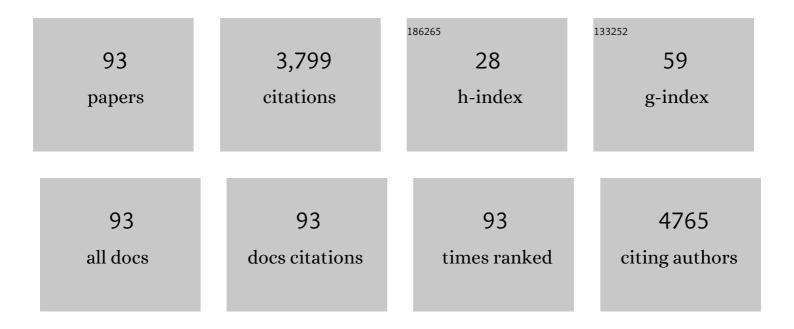
List of Publications by Year in descending order

Source: https://exaly.com/author-pdf/6336337/publications.pdf Version: 2024-02-01



#	Article	IF	CITATIONS
1	Improved Thermal Stability and Enhanced Thermoelectric Properties of p-Type BaCu2Te2 by Doping of Cl. ACS Applied Materials & Interfaces, 2022, 14, 5634-5642.	8.0	10
2	Half-Heusler-like compounds with wide continuous compositions and tunable p- to n-type semiconducting thermoelectrics. Nature Communications, 2022, 13, 35.	12.8	20
3	Origin of ductility in amorphous Ag2S0.4Te0.6. Applied Physics Letters, 2022, 120, .	3.3	11
4	Discovery of a Slater–Pauling Semiconductor ZrRu _{1.5} Sb with Promising Thermoelectric Properties. Advanced Functional Materials, 2022, 32, .	14.9	12
5	Synergistically Optimized Thermal Conductivity and Carrier Concentration in GeTe by Bi–Se Codoping. ACS Applied Materials & Interfaces, 2022, 14, 14359-14366.	8.0	9
6	Cu vacancy engineering of cage-compound BaCu2Se2: Realization of temperature-dependent hole concentration for high average thermoelectric figure-of-merit. Chemical Engineering Journal, 2022, 437, 135302.	12.7	6
7	Designing vacancy-filled Heusler thermoelectric semiconductors by the Slater-Pauling rule. Materials Today Energy, 2022, 27, 101035.	4.7	8
8	Entropy engineering: A simple route to both p- and n-type thermoelectrics from the same parent material. Materials Today Physics, 2022, 26, 100745.	6.0	6
9	Cubic Quaternary Silver Chalcogenide: A Promising Ductile Thermoelectric Inorganic. ACS Applied Energy Materials, 2022, 5, 8878-8884.	5.1	5
10	Tailoring the chemical bonding of GeTe-based alloys by MgB2 alloying to simultaneously enhance their mechanical and thermoelectric performance. Materials Today Physics, 2021, 16, 100308.	6.0	29
11	Influence of Ag substitution on thermoelectric properties of the quaternary diamond-like compound Zn2Cu3In3Te8. Journal of Materiomics, 2021, 7, 236-243.	5.7	7
12	Embedded in-situ nanodomains from chemical composition fluctuation in thermoelectric A2Cu3In3Te8 (AÂ= Zn, Cd). Materials Today Physics, 2021, 17, 100333.	6.0	8
13	Temperature-Dependent Band Renormalization in CoSb ₃ Skutterudites Due to Sb-Ring-Related Vibrations. Chemistry of Materials, 2021, 33, 1046-1052.	6.7	16
14	Stabilized cubic phase BiAgSe _{2â^'x} S _x with excellent thermoelectric properties <i>via</i> phase boundary engineering. Journal of Materials Chemistry C, 2021, 9, 6766-6772.	5.5	4
15	A general strategy for high-throughput experimental screening of promising bulk thermoelectric materials. Science China Materials, 2021, 64, 1751-1760.	6.3	8
16	Minimizing Thermal Conductivity for Boosting Thermoelectric Properties of Cu–Ni-Based Alloys through All-Scale Hierarchical Architectures. ACS Applied Energy Materials, 2021, 4, 5015-5023.	5.1	9
17	Optimization of electrical and thermal transport properties of layered Bi2O2Se via Nb doping. Journal of Materials Science, 2021, 56, 12732-12739.	3.7	3
18	Interfacial Decoration Tailoring the Thermoelectric Performance of TiCoNi _{<i>x</i>} Sb Half-Heusler Compounds. ACS Applied Energy Materials, 2021, 4, 7148-7156.	5.1	6

#	Article	IF	CITATIONS
19	Unveiling the origins of low lattice thermal conductivity in 122-phase Zintl compounds. Materials Today Physics, 2021, 21, 100480.	6.0	20
20	Precision grain boundary engineering in commercial Bi ₂ Te _{2.7} Se _{0.3} thermoelectric materials towards high performance. Journal of Materials Chemistry A, 2021, 9, 11442-11449.	10.3	26
21	The Electrical and Thermal Transport Properties of La-Doped SrTiO3 with Sc2O3 Composite. Materials, 2021, 14, 6279.	2.9	1
22	Anisotropic artificial synapse based on 2D ReS2 field-effect transistor. Applied Physics Letters, 2021, 119, 163102.	3.3	10
23	Enhancement of Thermoelectric Properties in n-type NbCoSn Half-Heusler Compounds via Ta Alloying. ACS Applied Energy Materials, 2021, 4, 12458-12465.	5.1	11
24	Highly Distorted Grain Boundary with an Enhanced Carrier/Phonon Segregation Effect Facilitates High-Performance Thermoelectric Materials. ACS Applied Materials & Interfaces, 2021, 13, 51018-51027.	8.0	13
25	Synergistically Optimizing Electrical and Thermal Transport Properties of ZrCoSb through Ru Doping. ACS Applied Energy Materials, 2021, 4, 13997-14003.	5.1	9
26	Optimizing Room-Temperature Thermoelectric Performance of n-Type Bi ₂ Te _{2.7} Se _{0.3} . ACS Omega, 2021, 6, 33883-33888.	3.5	11
27	Enhancement of the thermoelectric performance of InTe via introducing Cd dopant and regulating the annealing time. Journal of Alloys and Compounds, 2020, 813, 152210.	5.5	12
28	Effective Mass Enhancement and Thermal Conductivity Reduction for Improving the Thermoelectric Properties of Pseudoâ€Binary Ge ₂ Sb ₂ Te ₅ . Annalen Der Physik, 2020, 532, 1900390.	2.4	8
29	Tetrahedral Distortion and Thermoelectric Performance of the Ag-Substituted CuInTe ₂ Chalcopyrite Compound. ACS Applied Energy Materials, 2020, 3, 11015-11023.	5.1	16
30	Achieving High Thermoelectric Performance by Introducing 3D Atomically Thin Conductive Framework in Porous Bi ₂ Te _{2.7} Se _{0.3} arbon Nanotube Hybrids. Advanced Electronic Materials, 2020, 6, 2000292.	5.1	8
31	Excessive iodine addition leads to room-temperature superionic Cu2S with enhanced thermoelectric properties and improved thermal stability. Materials Today Physics, 2020, 15, 100271.	6.0	10
32	Dual-doping of ruthenium and nickel into Co ₃ O ₄ for improving the oxygen evolution activity. Materials Chemistry Frontiers, 2020, 4, 1390-1396.	5.9	26
33	Simultaneously increased carrier concentration and mobility in p-type Bi0.5Sb1.5Te3 throng Cd doping. Journal of Alloys and Compounds, 2020, 830, 154625.	5.5	23
34	Intermediate-level doping strategy to simultaneously optimize power factor and phonon thermal conductivity for improving thermoelectric figure of merit. Materials Today Physics, 2020, 15, 100250.	6.0	20
35	Suppressing the dynamic precipitation and lowering the thermal conductivity for stable and high thermoelectric performance in BaCu2Te2 based materials. Journal of Materials Chemistry A, 2020, 8, 5323-5331.	10.3	16
36	Hierarchical N-Doped Porous Carbons for Zn–Air Batteries and Supercapacitors. Nano-Micro Letters, 2020, 12, 20.	27.0	73

#	Article	IF	CITATIONS
37	Semiconductor glass with superior flexibility and high room temperature thermoelectric performance. Science Advances, 2020, 6, eaaz8423.	10.3	108
38	Precise Regulation of Carrier Concentration in Thermoelectric BiSbTe Alloys via Magnetic Doping. ACS Applied Materials & Interfaces, 2020, 12, 20653-20663.	8.0	37
39	High Thermoelectric Performance of Cu-Doped PbSe-PbS System Enabled by High-Throughput Experimental Screening. Research, 2020, 2020, 1736798.	5.7	18
40	Violation of the <i>T</i> ^{â^`1} Relationship in the Lattice Thermal Conductivity of Mg ₃ Sb ₂ with Locally Asymmetric Vibrations. Research, 2020, 2020, 4589786.	5.7	25
41	Realization of higher thermoelectric performance by dynamic doping of copper in n-type PbTe. Energy and Environmental Science, 2019, 12, 3089-3098.	30.8	127
42	Magnetoresistance and spin-torque effect in flexible nanoscale magnetic tunnel junction. Applied Physics Letters, 2019, 115, 052401.	3.3	2
43	Mechanochemical synthesis of multi-site electrocatalysts as bifunctional zinc–air battery electrodes. Journal of Materials Chemistry A, 2019, 7, 19355-19363.	10.3	53
44	Accelerating sample preparation of graded thermoelectric materials using an automatic powder feeding system. Advances in Manufacturing, 2019, 7, 278-287.	6.1	3
45	Enhanced room-temperature thermoelectric performance of p-type BiSbTe by reducing carrier concentration. RSC Advances, 2019, 9, 2252-2257.	3.6	4
46	Synergistic optimization of thermoelectric performance in p-type Ag2Te through Cu substitution. Journal of Materiomics, 2019, 5, 489-495.	5.7	33
47	Thermal stability of Ag9GaSe6 and its potential as a functionally graded thermoelectric material. Chemical Engineering Journal, 2019, 374, 494-501.	12.7	39
48	Enhanced and stabilized n-type thermoelectric performance in α-CuAgSe by Ni doping. Materials Today Physics, 2019, 10, 100095.	6.0	13
49	Manipulation of Ni Interstitials for Realizing Large Power Factor in TiNiSnâ€Based Materials. Advanced Electronic Materials, 2019, 5, 1900166.	5.1	32
50	Engineering the electronic structure of single atom Ru sites via compressive strain boosts acidic water oxidation electrocatalysis. Nature Catalysis, 2019, 2, 304-313.	34.4	757
51	Impurity tracking enables synthesis of TiFe1-Ni Sb half-Heusler compounds with high purity. Materials Today Physics, 2019, 11, 100173.	6.0	11
52	A ₂ Cu ₃ In ₃ Te ₈ (A = Cd, Zn, Mn, Mg): A Type of Thermoelectric Material with Complex Diamond-like Structure and Low Lattice Thermal Conductivities. ACS Applied Energy Materials, 2019, 2, 8956-8965.	5.1	17
53	Discovery of TaFeSb-based half-Heuslers with high thermoelectric performance. Nature Communications, 2019, 10, 270.	12.8	227
54	Realizing High Thermoelectric Performance in BaCu _{2–<i>x</i>} Ag _{<i>x</i>} Te ₂ through Enhanced Carrier Effective Mass and Point-Defect Scattering. ACS Applied Energy Materials, 2019, 2, 889-895.	5.1	26

#	Article	lF	CITATIONS
55	Effects of Se substitution for Te on electrical and thermal transport properties of BiCuTeO. Wuli Xuebao/Acta Physica Sinica, 2019, 68, 077201.	0.5	3
56	Increasing the thermoelectric power factor via Ag substitution at Zn site in Ba(Zn1-Ag)2Sb2. Journal of Alloys and Compounds, 2018, 745, 228-233.	5.5	5
57	Effective atomic interface engineering in Bi2Te2.7Se0.3 thermoelectric material by atomic-layer-deposition approach. Nano Energy, 2018, 49, 257-266.	16.0	49
58	Enhancing Thermoelectric Performance of PbSe by Se Vacancies. Journal of Electronic Materials, 2018, 47, 2584-2590.	2.2	8
59	Boosting the thermoelectric performance of PbSe through dynamic doping and hierarchical phonon scattering. Energy and Environmental Science, 2018, 11, 1848-1858.	30.8	163
60	Creation of Triple Hierarchical Micro-Meso-Macroporous N-doped Carbon Shells with Hollow Cores Toward the Electrocatalytic Oxygen Reduction Reaction. Nano-Micro Letters, 2018, 10, 3.	27.0	99
61	Discovery of High-Performance Thermoelectric Chalcogenides through Reliable High-Throughput Material Screening. Journal of the American Chemical Society, 2018, 140, 10785-10793.	13.7	134
62	Identifying the Key Role of Pyridinicâ€N–Co Bonding in Synergistic Electrocatalysis for Reversible ORR/OER. Advanced Materials, 2018, 30, e1800005.	21.0	394
63	Enhanced Average Thermoelectric Figure of Merit of the PbTe–SrTe–MnTe Alloy. ACS Applied Materials & Interfaces, 2017, 9, 8729-8736.	8.0	38
64	Significantly enhanced thermoelectric performance of Cu-doped p-type Bi _{0.5} Sb _{1.5} Te ₃ by a hydrothermal synthesis method. RSC Advances, 2017, 7, 41111-41116.	3.6	13
65	Effects of Mn substitution on thermoelectric properties of Culn 1â^'x Mn x Te 2. Chinese Physics B, 2017, 26, 097201.	1.4	6
66	Cd substitution in Zintl phase Eu5In2Sb6 enhancing the thermoelectric performance. Journal of Alloys and Compounds, 2017, 726, 618-622.	5.5	7
67	Optimized hetero-interfaces by tuning 2D SnS2 thickness in Bi2Te2.7Se0.3/SnS2 nanocomposites to enhance thermoelectric performance. Nano Energy, 2017, 39, 297-305.	16.0	74
68	Enhanced thermoelectric properties of BaZn ₂ Sb ₂ via a synergistic optimization strategy using co-doped Na and Sr. Journal of Materials Chemistry A, 2016, 4, 12119-12125.	10.3	19
69	Enhanced thermoelectric performance in PbSe-SrSe solid solution by Mn substitution. Journal of Alloys and Compounds, 2016, 687, 765-772.	5.5	15
70	Hierarchical Nanoarrays: Hierarchical α-MnO2Tube-on-Tube Arrays with Superior, Structure-Dependent Pseudocapacitor Performance Synthesized via a Selective Dissolution and Coherent Growth Mechanism (Adv. Mater. Interfaces 8/2016). Advanced Materials Interfaces, 2016, 3, .	3.7	0
71	2D hetero-nanosheets to enable ultralow thermal conductivity by all scale phonon scattering for highly thermoelectric performance. Nano Energy, 2016, 30, 780-789.	16.0	54
72	EO polymer at cryogenic temperatures. Electronics Letters, 2016, 52, 1703-1705.	1.0	4

#	Article	IF	CITATIONS
73	Eutectic microstructures and thermoelectric properties of MnTe-rich precipitates hardened PbTe. Acta Materialia, 2016, 111, 202-209.	7.9	32
74	Hierarchical αâ€MnO ₂ Tubeâ€onâ€Tube Arrays with Superior, Structureâ€Dependent Pseudocapacitor Performance Synthesized via a Selective Dissolution and Coherent Growth Mechanism. Advanced Materials Interfaces, 2016, 3, 1500761.	3.7	8
75	Thermoelectric Properties of Heavily Doped n-type Pb1â^'x Y x Te Compounds. Journal of Electronic Materials, 2015, 44, 3556-3562.	2.2	6
76	100 Gbit/s OOK using a silicon-organic hybrid (SOH) modulator. , 2015, , .		12
77	Improved photovoltaic performance of dye-sensitized solar cells by carbon-ion implantation of tri-layer titania film electrodes. Rare Metals, 2015, 34, 34-39.	7.1	8
78	Enhanced thermoelectric properties of p-type Ag ₂ Te by Cu substitution. Journal of Materials Chemistry A, 2015, 3, 10303-10308.	10.3	49
79	Discrete Li-occupation versus pseudo-continuous Na-occupation and their relationship with structural change behaviors in Fe2(MoO4)3. Scientific Reports, 2015, 5, 8810.	3.3	42
80	Effects of Ag-ion implantation on the performance of DSSCs with a tri-layer TiO ₂ film. RSC Advances, 2014, 4, 56318-56322.	3.6	17
81	Time-, Energy-, and Phase-Resolved Second-Harmonic Generation at Semiconductor Interfaces. Journal of Physical Chemistry C, 2014, 118, 27981-27988.	3.1	19
82	Three-dimensional self-branching anatase TiO ₂ nanorods: morphology control, growth mechanism and dye-sensitized solar cell application. Journal of Materials Chemistry A, 2014, 2, 16030-16038.	10.3	21
83	Synthesis of highly crystalline Bi ₂ Te ₃ nanotubes and their enhanced thermoelectric properties. Journal of Materials Chemistry A, 2014, 2, 12821.	10.3	45
84	High thermoelectric performance of Ge1â^'xPbxSe0.5Te0.5 due to (Pb, Se) co-doping. Acta Materialia, 2014, 74, 215-223.	7.9	28
85	Phase separation and thermoelectric properties of Ag2Te-doped PbTe0.9S0.1. Acta Materialia, 2012, 60, 7241-7248.	7.9	14
86	Stable micro-feeding of fine powders using a capillary with ultrasonic vibration. Powder Technology, 2011, 214, 237-242.	4.2	30
87	Highly Efficient Diels–Alder Crosslinkable Electroâ€Optic Dendrimers for Electricâ€Field Sensors. Advanced Functional Materials, 2007, 17, 2557-2563.	14.9	73
88	Tunable Fabry-Perot Filters using Electro-Optic Hybrid Sol-Gel. , 2006, , .		0
89	Highly Efficient and Thermally Stable Electro-optic Polymer from a Smartly Controlled Crosslinking Process. Advanced Materials, 2003, 15, 1635-1638.	21.0	72
90	Microcathodoluminescence spectroscopy of defects in Bi2O3-doped ZnO grains. Journal of Applied Physics, 2002, 92, 5072-5076.	2.5	7

#	Article	IF	CITATIONS
91	Design, Synthesis, and Properties of Highly Efficient Side-Chain Dendronized Nonlinear Optical Polymers for Electro-Optics. Advanced Materials, 2002, 14, 1763-1768.	21.0	124
92	Microstructure evolution and grain growth in the sintering of 3Y–TZP ceramics. Journal of Materials Science, 1998, 33, 5301-5309.	3.7	48
93	Effect of filler porosity on the abrasion resistance of nanoporous silica gel/polymer composites. Dental Materials, 1998, 14, 29-36.	3.5	37